Planetary Nebulae: Multi-Wavelength Probes of Stellar and Galactic Evolution
Proceedings IAU Symposium No. 323, 2016
X. Liu, L. Stanghellini & A. Karakas, eds.

doi:10.1017/S1743921317001466

XSHOOTER spectroscopy of the enigmatic PN Lin49 in the SMC

Masaaki Otsuka[1], Francisca Kemper[1], Marcelo L. Leal-Ferreira[2], Isabel Aleman[2], Jeronimo Bernard-Salas[3], Jan Cami[4,5], Bram B. Ochsendorf[6], Els Peeters[4,5] and Peter Scicluna[1]

[1]ASIAA, 11F of Astronomy-Mathematics Building, AS/NTU. No.1, Sec. 4, Roosevelt Rd, Taipei 10617, Taiwan, R.O.C. email: otsuka@asiaa.sinica.edu.tw (MO)

[2]Leiden Observatory, University of Leiden, PO Box 9513, 2300 RA, Leiden, The Netherlands

[3]Department of Physical Sciences, The Open Univ., Milton Keynes, MK7 6AA, UK

[4]Department of Physics & Astronomy, The Univ. of Western Ontario, London, ON N6A 3K7, Canada

[5]SETI Institute, 189 Bernardo Ave, Suite 100, Mountain View, CA 94043, USA

[6]Space Telescope Science Institute, 3700 San Martin Drive, Baltimore, MD 21218, USA,

Abstract. We performed a detailed spectroscopic analysis of the fullerene C_{60}-containing planetary nebula (PN) Lin49 in the Small Magellanic Cloud (SMC). Lin49 is a C-rich and metal-deficient PN ($Z\sim0.0006$) and its nebular abundances are in agreement with the AGB model for the initially $1.25\,M_{\odot}$ stars with the metallicity $Z = 0.001$. By stellar absorption fitting with TLUSTY, we derived stellar abundances, effective temperature, and surface gravity. We constructed the photoionization model with CLOUDY in order to investigate physical conditions of Lin49. The model with the 0.005-0.1 μm radius graphite and a constant hydrogen density shell could not fit the $\sim$1-5 μm spectral energy distribution (SED) owing to the strong near-IR excess. We propose that the near-IR excess indicates (1) the presence of extremely small carbon molecules or (2) the presence of high-density structure surrounding the central star.

Keywords. infrared: ISM, ISM: abundances, dust, molecules, planetary nebulae: individual (Lin49), stars: abundances

1. C_{60}-containing PN Lin49 in the SMC

Recently, *Spitzer*/IRS mid-IR spectrum revealed that Lin49 is a C-rich dust PN, showing strong C_{60} resonances at 17.4 and 18.9 μm and similar dust features such as the broad 11 μm and 30 μm features seen in the other C_{60}-containing Magellanic Cloud PNe Sloan *et al.* (2014). However, physical properties of the central star and the dusty nebula had been unknown. Therefore, we characterized Lin49 through abundance analysis, stellar absorption fitting, and photoionization modeling based on our own ESO/VLT X-SHOOTER UV to near-IR spectrum, the archived *Spitzer*/IRS spectrum, and the UV to mid-IR photometry data.

2. Nebular abundances and Stellar absorption line analysis

The resultant elemental abundances are listed in Table 1. With the XSHOOTER and *Spitzer*/IRS spectra, we determined the nebular abundances of nine elements. We found that the nebular abundances are in agreement with the AGB star nucleosynthesis model for the initially $1.25\,M_{\odot}$ and the metallicity $Z_{\odot}/20$ stars by Fishlock *et al.* (2014).

Table 1. Elemental abundances ($\log_{10}\epsilon(\mathrm{H}) = 12$). The values in the last two columns are the predictions in the AGB models by Fishlock *et al.* (2014) for initially $1.0\,M_\odot$ and $1.25\,M_\odot$ stars with $Z = 0.001$.

X	$\log_{10}\epsilon(\mathrm{X})$	$\log_{10}\epsilon(\mathrm{X}_\odot)$	[X/H]	$\log_{10}\epsilon(\mathrm{X}_{1.0\,M_\odot\mathrm{model}})$	$\log_{10}\epsilon(\mathrm{X}_{1.25\,M_\odot\mathrm{model}})$
He	10.80 - 11.01	10.93 ± 0.01	−0.13 - +0.08	10.99	11.01
C	8.46 ± 0.24	8.39 ± 0.04	+0.07 ± 0.25	8.06	8.56
N	6.93 ± 0.02	7.86 ± 0.12	−0.93 ± 0.12	7.15	7.26
O	8.11 ± 0.01	8.73 ± 0.07	−0.62 ± 0.07	7.58	7.68
Ne	7.18 ± 0.05	8.05 ± 0.10	−0.89 ± 0.11	6.89	7.37
S	6.02 ± 0.01	7.16 ± 0.02	−1.15 ± 0.02	5.99	6.00
Cl	4.03 ± 0.05	5.25 ± 0.06	−1.22 ± 0.08	4.07	4.08
Ar	5.48 ± 0.11	6.50 ± 0.10	−1.02 ± 0.15	5.27	5.28
Fe	4.55 ± 0.04	7.46 ± 0.08	−2.91 ± 0.09	6.37	6.38

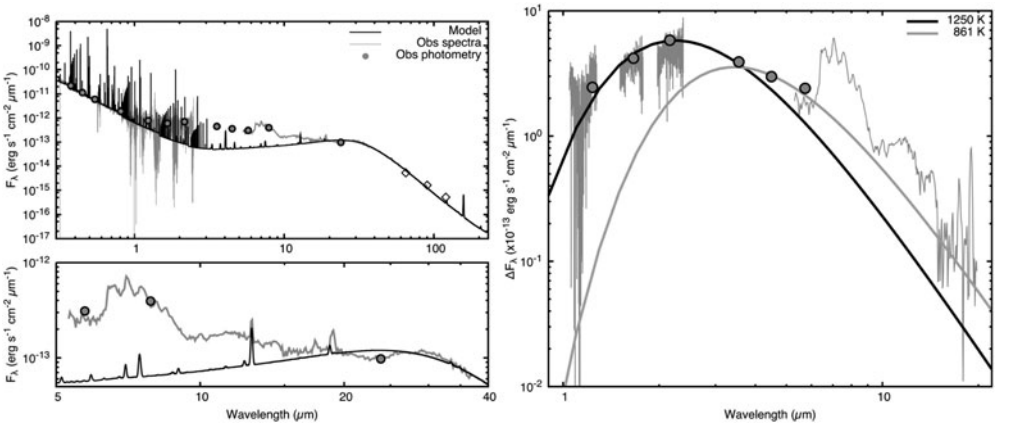

Figure 1. (*left panels*) (upper) Comparison between the CLOUDY model and observational data. The squares at 65, 90, and 120 μm are the *predicted* flux densities calculated by fitting the broad 30 μm feature. (lower) Closed-up plots for mid-IR wavelength. (*right panel*) Near-IR excess. The grey lines and the circles are the residual flux densities (ΔF_λ) between the observed X-SHOOTER and *Spitzer*/IRS spectra and photometry bands and the corresponding values obtained from the CLOUDY model.

We fit stellar absorption lines with the O-type star grid model OStar2002 by Lanz & Hubeny (2003) using the non-LTE model stellar atmospheres modeling code TLUSTY by Hubeny (1988). We determined the effective temperature (T_{eff}) of 30 500 ± 500 K, the surface gravity ($\log g$) of 3.29 ± 0.06 cm s^{-2}, and ϵ(He,C,N,O,Si) of 10.9 ± 0.3, 9.0 ± 0.3, 7.6 ± 0.3, 8.6 ± 0.1, and 6.8 ± 0.3, respectively.

3. Photoionization modeling; finding of the near-IR excess

Using the photoionization code CLOUDY (Ferland *et al.* 2013), we investigated physical conditions of Lin49. As the SED of the ionization/heating source, we used the central star's spectrum synthesized by the TLUSTY and varied its intrinsic luminosity (L_*) to match the observed nebular elemental abundances, gas emission line fluxes, and broad band fluxes/flux densities. We supposed that the infrared continuum is due to graphite grains; we adopted the radius a = 0.005-0.1 μm and the $a^{-3.5}$ size distribution. We derived the gas and dust masses of $0.11\,M_\odot$ and $4.3\times10^{-5}\,M_\odot$, respectively. The dust temperature is in the range from 79 K to 825 K. We determined the core-mass of 0.53-$0.57\,M_\odot$. The location of the derived L_* and T_{eff} on evolutionary tracks of post AGB

https://doi.org/10.1017/S1743921317001466 Published online by Cambridge University Press

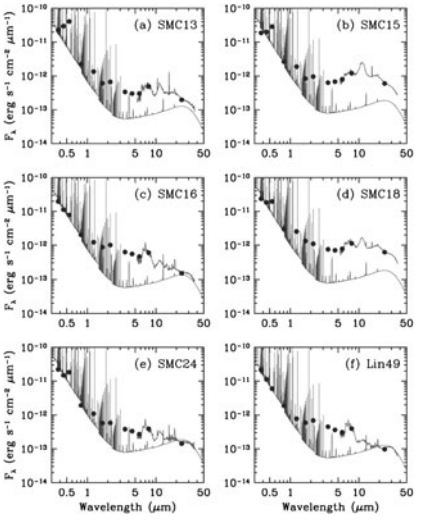

Figure 2. SED plots of SMC C_{60} PNe. The filled circles are the de-reddened photometric data. In each panel, we compare with the resultant SED of Lin49 presented in Fig 1 left. In each panel, Lin49's SED is scaled to the observed de-reddened flux density of each PN at the I_c band.

stars with $Z = 0.001$ of Vassiliadis & Wood (1994) indicates that the initial mass is 1.0-1.5 $M_{\odot}$, consistent with our inference from the nebular abundances.

In Fig. 1 left, we present the observed and the modeled SEDs. The predicted SED could not fit the near-IR SED owing to the strong near-IR excess. To focus on the near-IR excess, we examined the differential spectra and photometry points between the observations and the CLOUDY model (Fig. 1 right); the near-IR excess peaks at ∼2-3 μm and its SED can be fitted by a single blackbody temperature of 1250 K.

4. Interpretations for the near infrared excess

In Fig. 2, we plot the observed data of SMC C_{60} PNe and compare their SED plots with the scaled Lin49's model SED. The near-IR excess is a common feature in SMC C_{60} PNe. The near-IR excess might hold the important information to disclose the C_{60} formation process in PNe. The near-IR excess in these PNe might indicate case 1: the presence of small carbon clusters and also fullerene precursors (in the XSHOOTER K-band spectrum of Lin49, we did not detect any H_2 and CO lines) or case 2: the presence of a sub-structure surrounding the central star.

4.1. *Stochastic heating by extremely small particles*

For small molecules, a single photon energy E_{ph} produces the difference between the maximum and minimum temperatures $\Delta T = E_{ph}/3Nk$, where N is the number of the atoms in a molecule and k is the Boltzmann constant. We obtained a N of ∼39. As a pragmatic problem, with grains composing of 39 C-atoms only, it is difficult to reproduce the observed broad continuous near-IR excess feature seen in Lin49; to get a continuum like behavior, enough interacting vibrational modes are necessary.

4.2. *The presence of a sub-structure surrounding the central star*

Therefore, the near-IR excess would be due to the presence of a sub-structure surrounding the central star such a disc. We can fit the near-IR excess in Lin49 (Fig. 3 right), supposing the two density shells as explained in Fig. 3 left. Since the temperature in the disc

https://doi.org/10.1017/S1743921317001466 Published online by Cambridge University Press

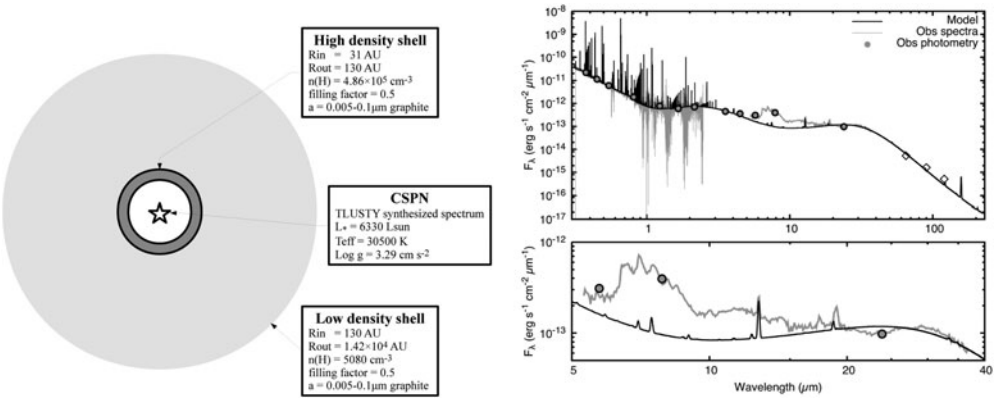

Figure 3. (*left panel*) The explanation of the two density shell model. The central star is located in the geometrical center of two spherical nebulae, so called *high density shell* and *low density shell*. As the ionization and heating source, we used the spectrum of the central star (CSPN) synthesized by the TLUSTY fitting. (*right two panels*) (upper) Comparison between the observed SED plots and the predicted SED by the two density shell model. (lower) Closed-up plot for mid-IR wavelength. The dust temperature was in the range of 79 K to 1453 K. The lines and symbols in both of panels are as defined in Fig. 1 left.

decreases with increasing radius, at the inner radius of the disc only the elements such Fe with a high condensation temperature are caught in grains. Indeed, the Fe abundance of Lin49 is extremely deficient ([Fe/H] = –2.9) compared to heavy α-elements (e.g., [Ar/H] = –1.0). If Lin49 has a disc, the large carbon molecules such as fullerene were relatively easily formed. Detailed discussions are found in Otsuka *et al.* (2016).

5. Future works

The near-IR excess is a common feature in SMC C_{60} PNe. However, since there are no available near-IR spectra of these SMC C_{60} PNe to confirm the near-IR excess spectroscopically, it is still far from the firm conclusion on the C_{60} formation in these SMC PNe. It is worth investigating the SMC C_{60} PNe in order to understand the C_{60} formation in the circumstellar environment; the well determined distance to the SMC allows us to accurately determine the luminosity of the central star, the size of the nebula, and physical conditions of the gas, dust, and C_{60} in the nebula, and then clarify the current evolutionary stage of the central star and estimate the initial mass. Based on the larger sample, we can conclude that the near-IR excess indicates the presence of a sub-structure such as a disc surrounding the central star and the fullerene was efficiently made within this disc. By investigating the near-IR excess of the SMC C_{60} PNe, we can find what conditions are essential in the C_{60} formation in PNe.

References

Ferland, G. J., Porter, R. L., van Hoof, P. A. M., *et al.* 2013, *RMxAA*, 49, 137
Fishlock, C. K., Karakas, A. I., Lugaro, M., & Yong, D. 2014, *ApJ*, 797, 44
Hubeny, I. 1988, *Computer Physics Communications*, 52, 103
Lanz, T. & Hubeny, I. 2003, *ApJS*, 146, 417
Otsuka, M., Kemper, F., Leal-Ferreira, M. L., *et al.* 2016, *MNRAS*, 462, 12
Sloan, G. C., Lagadec, E., Zijlstra, A. A., *et al.* 2014, *ApJ*, 791, 28
Vassiliadis, E. & Wood, P. R. 1994, *ApJS*, 92, 125

https://doi.org/10.1017/S1743921317001466 Published online by Cambridge University Press

Discussion

SLOAN: The Fe depletion makes me think of the solid Fe proposed by IainMcDonald to explain a near-IR excess in different systems. Have you tried this?

OTSUKA: We have no optical constant of the pure Fe grains in the wavelength from X-ray. The X-ray-UV energy of the CSPN is important heating source for the grains. At this moment, we cannot test a model including the graphite and the pure Fe grains. To verify whether near-IR excess in PNe is mainly from the Fe dust thermal emission, the high-resolution J or I and K band images taken with AO-system and the 2-D Fe abundance map by slit-scan observation are useful. Although we cannot obtain such data for Lin 49 in the SMC, we can test Galactic C-rich PNe showing near-IR excess.

https://doi.org/10.1017/S1743921317001466 Published online by Cambridge University Press